Int. J. Heat Mass Transfer. Vol. 19, pp. 33–40. Pergamon Press 1976. Printed in Great Britain

THE EFFECT OF WALL TEMPERATURE ON THE GROWTH AND SEPARATION OF THE LAMINAR BOUNDARY LAYER OF A SPHERE

M. C. SMITH and M. C. POTTER
Mechanical Engineering, Michigan State University, East Lansing, MI 48824, U.S.A.

and

S. KAPUR
Ranaqu Industries, New Delhi, India

(*Received* 6 *September* 1974)

Abstract—Results are given for the numerical integration of the laminar boundary-layer equations for a sphere, up to the separation point, and for experiments on a constant temperature sphere at a low Reynolds number in water. Both experimental and numerical results show that increasing the sphere temperature above that of the surrounding water shifts the laminar separation point slightly to the rear. The effect of buoyancy is very small. The influence of heating on velocity and temperature profiles is presented.

The results are compared with results obtained by others for a two-dimensional cylinder. The dimensionless heat transfer and skin friction as functions of the dimensionless distance along the wall to separation are found to be similar to those obtained for the cylinder. Correlations as a function of free stream and wall Prandtl number ratio are obtained both for potential flow about the sphere and for an experimental velocity distribution which reflects the effect of separation. These are compared with the correlation for a circular cylinder.

NOMENCLATURE

C, μ/μ_∞;

C_f, skin friction coefficient, $\dfrac{\tau_w}{1/2\rho_m U_e^2(\xi)}$;

C_p, specific heat [cm^2/s^2 deg];

G, dimensionless temperature, $(T-T_w)/(T_m-T_w)$;

L, generalized non-dimensionalizing length [cm];

Nu_ξ, Nusselt number, $\dfrac{\xi(\partial T/\partial y)w}{(T_m-T_w)}$;

P, $\dfrac{\xi}{U_e}\dfrac{dUe}{d\xi}$;

Pr, fluid Prandtl number, $\dfrac{C_p\mu}{k}$;

R, $\dfrac{\xi}{r_0}\dfrac{dr_0}{d\xi}$;

R_ξ, Reynolds number, $\rho_m U_e(\xi)\xi/\mu_m$;

T, temperature [deg C];

U_e, velocity component in the x direction external to the boundary layer [cm/s];

U_∞, velocity at infinity [cm/s];

c, sphere radius [cm];

f, dimensionless stream function (equation 12);

g, dimensionless temperature T/T_∞;

g_x, acceleration of gravity in the x direction [cm/s^2];

k, fluid thermal conductivity [g cm/s^3 deg];

m, exponent for velocity distribution;

p, fluid pressure [g/cm s^2];

r, distance from the axis of symmetry [cm];

r_0, distance from the axis of symmetry to the wall of the sphere;

u, v, velocity components in the boundary layer parallel and normal to the wall [cm/s];

x, y, coordinates along and normal to the wall [cm];

ΔT, temperature difference between sphere wall and fluid at infinity.

Greek symbols

α, angle from forward stagnation point [deg];

β, coefficient of fluid expansion [1/deg C];

δ, boundary-layer thickness [cm];

μ, fluid viscosity [g/cm s];

ξ, η, dimensionless coordinates (equation 11);

ρ, fluid density [g/cm^3];

τ, shear stress at the wall [g/cm s^2].

Subscripts

e, external to boundary layer;

$0, w$, at the wall;

s, separation point;

∞, m, fluid at infinity;

0, at $\xi = 0$;

ξ, varying with ξ;

D, reference diameter;

T, temperature;

V, velocity.

INTRODUCTION

THE LAMINAR boundary layer can sustain only a small adverse pressure gradient without separating from a solid surface. It is desirable in many instances to prevent such a separation; thus, many studies have been made to determine the effect on separation of blowing, suction and the pressure gradient. Since the governing fluid properties in the laminar, incompressible boundary layer are the fluid viscosity, thermal conductivity and density, their variation also can be expected to affect separation. As these properties are temperature dependent, variations are most easily accomplished in the boundary layer by maintaining a temperature difference between the solid wall and the fluid. This discussion is concerned with the effect of this temperature difference in the specific instance of water flowing around a sphere.

The effect on laminar separation of heat transfer from gases to the boundary has been studied by Morduchow [1], Stewartson [2] and Illingworth [3], among others, with the general conclusion that cooling the gas tends to "delay" separation. Equivalently, a larger adverse pressure gradient is required to maintain the same separation point when the gas is cooled. It is noted that most of these studies are restricted to the similarity solutions where $U_e/U_\infty = x^m$. Further studies by Illingworth [3], Gadd [4], Curle [5] and Poots [6] for $U_e/U_\infty = 1-x$ have confirmed the result that cooling of the gas delays separation, and, in addition, studies by Baxter and Flügge-Lotz [7] and Fannelop and Flügge-Lotz [8] of the effect of heating the gas show the opposite effect on separation.

Since the viscosity of liquids is reduced by heating, opposite to the effect in gases, it would be expected that heating liquids would delay separation. Studies by Schuh [9], Hanna and Myers [10], and Johnson [11] have shown that heating reduces skin friction. The study by Schuh [9] contains the conclusion that heating will delay separation although no quantitative results are given. One experimental study by Brown [12] has shown that a heated sphere in a liquid flow will experience a shift in the separation point from about 84° from the forward stagnation point with no heating to about 100° with heating. As this result was incidental to the main purpose of the study, details are not given.

In this study the sphere laminar boundary layer is treated numerically and experimentally to more fully determine the effect on separation of temperature difference between the boundary and the liquid. The numerical results naturally include details concerning the temperature and velocity profiles in the boundary layer. Flat plate results were obtained as a partial check on the numerical calculations; they coincide with those reported by Poots and Raggett [13] and are not included herein.

MATHEMATICAL FORMULATION

Axisymmetric steady flow about a body of revolution is considered, the flow past a flat plate being obtained by letting the body radius go to a large constant. The conservation laws for energy, momentum and mass are used for this configuration, and, in addition, the dependence of fluid viscosity, density, and Prandtl number on temperature are specified. The explicit dependence of thermal conductivity on temperature is not used, as the variation is only about 15 per cent compared with a 400 per cent variation in viscosity and an even greater variation in Prandtl number over the range of temperature herein considered. Buoyancy, or the effect of gravity, is included even though its influence may be expected to be small; the density is much less sensitive to temperature than is the viscosity.

As a result of axisymmetry only x, y coordinates and u, v velocity components need be considered. The equations to be used have been developed by Millikan [14] and are given for convenient reference as

$$\frac{1}{r}\left[\frac{\partial}{\partial x}(ru)+\frac{\partial}{\partial y}(rv)\right]=0 \tag{1}$$

$$\rho\left[u\frac{\partial u}{\partial x}+v\frac{\partial u}{\partial y}\right]=-\frac{dp}{dx}+\rho g_x+\frac{\partial}{\partial y}\left(\mu\frac{\partial u}{\partial y}\right)+\frac{\mu}{r}\frac{\partial r}{\partial y}\frac{\partial u}{\partial y} \tag{2}$$

$$\rho C_p\left[u\frac{\partial T}{\partial x}+v\frac{\partial T}{\partial y}\right]=k\frac{\partial^2 T}{\partial y^2}+\frac{k}{r}\frac{\partial r}{\partial y}\frac{\partial T}{\partial y}. \tag{3}$$

Fluid properties k and C_p are considered constant.

Viscous dissipation, compression effects, and transverse curvature terms are neglected in obtaining equations (1)–(3). These latter terms do not exist for the flat plate and are known to be negligible for the sphere. For a thin boundary layer, r can be replaced by $r_0(x)$ in equation (1) and the equations become

$$\frac{\partial}{\partial x}(r_0 u)+r_0\frac{\partial v}{\partial y}=0 \tag{4}$$

$$\rho\left[u\frac{\partial u}{\partial x}+v\frac{\partial u}{\partial y}\right]=-\frac{dp}{dx}+\rho g_x+\frac{\partial}{\partial y}\left(\mu\frac{\partial u}{\partial y}\right) \tag{5}$$

$$\rho C_p\left[u\frac{\partial T}{\partial x}+v\frac{\partial T}{\partial y}\right]=k\frac{\partial^2 T}{\partial y^2}. \tag{6}$$

The boundary conditions are

$$\begin{aligned} &y=0, \quad u=v=0\\ &y=0, \quad T=T_w=\text{given}\\ &y=\delta_U, \quad u=U_e(x)\\ &y=\delta_T, \quad T=T_\infty. \end{aligned} \tag{7}$$

The stream function ψ can be defined by

$$\begin{aligned} u&=\frac{1}{r_0}\frac{\partial}{\partial y}(\psi r_0)=\frac{\partial \psi}{\partial y}\\ v&=-\frac{1}{r_0}\frac{\partial}{\partial x}(\psi r_0)=-\frac{\partial \psi}{\partial x}-\frac{\psi}{r_0}\frac{\partial r_0}{\partial x}. \end{aligned} \tag{8}$$

This eliminates the need for the continuity equation. The momentum equation then becomes

$$\rho_\infty\left[\frac{\partial \psi}{\partial y}\frac{\partial^2 \psi}{\partial x \partial y}-\frac{\partial \psi}{\partial x}\frac{\partial^2 \psi}{\partial y^2}-\frac{\psi}{r_0}\frac{\partial r_0}{\partial x}\frac{\partial^2 \psi}{\partial y^2}\right]$$
$$=\rho_\infty U_e\frac{dU_e}{dx}+\rho_\infty \beta g_x(T-T_\infty)+\frac{\partial}{\partial y}\left(\mu\frac{\partial^2 \psi}{\partial y^2}\right) \tag{9}$$

wherein Euler's equation has been used as

$$\frac{dp}{dx}+\rho_\infty U_e\frac{dU_e}{dx}+g_x\rho_\infty=0 \tag{10}$$

as has the approximation $\rho=\rho_\infty[1-\beta(T-T_\infty)]$.

The modified Howarth–Dorotnitsyn transformation is convenient to use. Thus, introducing

$$\xi=x/L,\quad \eta=\left(\frac{U_e\rho_\infty}{\mu_\infty L}\right)^{1/2}y \tag{11}$$

and the dimensionless stream function f

$$f(\xi,\eta)=\left(\frac{\rho_\infty}{LU_e\mu_\infty\xi}\right)^{1/2}\psi \tag{12}$$

the momentum and energy equations may be obtained in dimensionless form. Using the definitions for C, P, R, Pr_∞ and g, the dimensionless momentum and energy equations become

$$(Cf'')'+P(1-f'^2)+\left(\frac{P+1}{2}+R\right)ff''+\frac{\xi L}{U_e^2}g_x\beta(T-T_\infty)=\xi\left(f'\frac{\partial f'}{\partial\xi}-f''\frac{\partial f}{\partial\xi}\right) \tag{13}$$

$$\frac{1}{Pr_\infty}\frac{\partial}{\partial\eta}(g')+\left(\frac{P+1}{2}+R\right)fg'=\xi\left(f'\frac{\partial g}{\partial\xi}-g'\frac{\partial f}{\partial\xi}\right) \tag{14}$$

with boundary conditions

$$\begin{aligned}\eta=0,&\quad f'=f=0\\&\quad g=T_w/T_\infty\\ \eta\to\infty,&\quad f'=1\\&\quad g=1.\end{aligned} \tag{15}$$

These equations have been used previously by Clutter and Smith [15]. The variations of ρ, Pr and μ with temperature have been taken from [15] and are:

$$\begin{aligned}\frac{\mu}{\mu_r}&=1/[35{\cdot}16-106{\cdot}98(T/T_r)+107{\cdot}77(T/T_r)^2\\&\quad-40{\cdot}6(T/T_r)^3+5{\cdot}64(T/T_r)^4]\\ \frac{\rho}{\rho_r}&=0{\cdot}8039+0{\cdot}4615(T/T_r)-0{\cdot}2869(T/T_r)^2\\&\quad+0{\cdot}0235(T/T_r)^3\\ \frac{Pr}{Pr_r}&=1/[73{\cdot}38-208{\cdot}75(T/T_r)+197{\cdot}76(T/T_r)^2\\&\quad-68{\cdot}86(T/T_r)^3+7{\cdot}48(T/T_r)^4]\end{aligned} \tag{16}$$

where the subscript r implies reference values taken at 32°F (491·69°R in equation (16)) for the water properties.

Solution of these equations is obtained by combining the differential-difference equations technique of Hartree and Womersley [16] with finite difference formulas in two directions. The wall boundary conditions are varied in an initial value solution to meet the required flow conditions for large η. This method circumvents the need to define "large η", but requires a trial and error variation on the wall value with a judgment in matching large η values.

The solution method requires a first estimate on the velocity and temperature profiles at the first x-station. The momentum equation is then satisfied and the solution is used to find the new temperature profile from the energy equation. This process is repeated until convergence occurs. Details of the solution method vary little from those described in [15]. Conventional integration schemes are used with variable step size in both η and ξ.

EXPERIMENTS

The experiments were conducted to provide an estimate of the effect on the separation point of heating a sphere. A brass sphere was placed in a square horizontal test section of a loop designed to circulate water. The sphere was heated electrically by means of a heating element placed inside the hollow brass sphere. The temperature difference between the water upstream from the sphere and the wall of the sphere was measured with the use of thermocouples. Hydrogen bubbles generated by a fine wire placed on the surface of the sphere were used to visualize the flow around the unheated sphere, while the shadowgraph method was employed when the sphere was heated.

Heated sphere

The 7·61 cm (±0·01) (3 in) external diameter hollow brass sphere consisted of two hemispheres joined together. The wall of the sphere was 0·633 cm (0·25 in) thick resulting in a constant temperature sphere. The heating element consisted of 6·4 m of Nichrome wire with asbestos insulation.

Four, 30-gauge iron–constantin thermocouples were soft-soldered into the inside wall of the sphere; No. 1 at 70°, No. 2 at 45°, No. 3 at 0°, No. 4 at 315° (all angles measured clockwise from the forward stagnation point). The thermocouples, when imbedded into the wall, were 0·159 cm from the outside surface. Since the temperature difference between the upstream water and the wall of the sphere is required, a thermocouple was placed upstream of the sphere and used as the reference junction. The heating element lead wires and the thermocouple wires passed through the Plexiglas support tube at the rear.

The brass sphere was marked at 2° intervals between 80° and 100° measured from the forward stagnation point and was covered with a thin coat of varnish, which insulated the sphere from the fine wire which generated the hydrogen bubbles. The hollow sphere was filled with water before it was placed into the test section. The water served to improve the heat transfer to the interior walls of the sphere.

Water flow system

The water flow loop consisted of a variable flow rate pump, two tanks and a 25·4 cm square plexiglas test section. Water was circulated by a centrifugal pump. The walls of the upstream and downstream tanks were lined with stainless steel sheets. The upstream tank contained three straightening sections. The first of these contained glass marbles sandwiched between two stainless steel screens; the second, a fine mesh stainless steel screen; and the third, a honeycomb constructed by placing 7·6-cm long, 0·5-cm dia plastic soda straws between two stainless steel screens. The

honeycomb was placed at the inlet of the square test section, so as to insure uniform velocity profiles in the test section. No measurement was made of the low free stream fluctuation level. However, hydrogen bubble traces showed no observable fluctuations. The piping used to transport water from the downstream tank to the upstream tank through the pump was made of polyvinyl chloride, a plastic material.

Care was taken to maintain the water as free from impurities as possible. Before any tests were made, the water in the test loop was passed through a water filter at low speeds for at least 12 h.

Flow visualization and procedure

The two visualization techniques, the hydrogen bubble method and the shadowgraph method, used in the present work will not be discussed at any length because they have been used in the past by many researchers. Some comments will be made, however, of the techniques used in the present study.

The hydrogen bubble method consists of using a fine wire as one end of a DC circuit to electrolyze the water. The tiny bubbles thus formed are visualized by means of an appropriate light source placed outside the test section. A 0·0025 cm platinum wire was used to generate the hydrogen bubbles. A spectra-Physics laser beam passed through a cylindrical lens was used as a light source. The platinum wire was stretched across the top half of the meridian plane. Thus, the hydrogen bubbles were generated next to the surface of the sphere, in the boundary layer and the wake region.

The shadowgraph method is based on the phenomenon that light passing through a density gradient in a fluid is deflected. It measures the second derivative, therefore allowing visualization of only those parts of the flow where the density gradient change is sufficiently large. The shadowgraph system consists of a bright light source, a colliminating lens, and a viewing screen.

Photographs were taken of the region near the separation point using the hydrogen bubble method and of the whole flow field around the sphere using the shadowgraph method. The laser beam used to visualize the hydrogen bubbles was not photographed directly; a video recording was made with a TV camera installed with a 130 mm lens. The video pictures projected on the TV screen were then photographed. The shadowgraph pictures were directly photographed.

The test loop was filled with soft water and the brass sphere was installed in the test section. The flow of water through the test section was about 0·8 cm/s. The Reynolds number, based on the diameter of the sphere, was thus 7500. This low Reynolds number assured a laminar flow in the boundary layer prior to separation.

Before the sphere was heated, the hydrogen bubbles were generated and photographs taken to insure the occurrence of laminar separation (about 84°). The power to the heating element inside the sphere was then adjusted to provide the desired temperature difference between the water upstream of the sphere and the wall of the sphere. The shadowgraph pictures were taken for various temperature differences.

Prior to making any tests, the sphere was heated to check the uniformity of the temperature of the sphere wall. All the thermocouples (1–4) were used to check that the wall temperature was essentially constant. When the sphere was heated, two thermocouples (2 and 4) were used to determine the temperature difference between the water upstream and the wall of the sphere. The sphere reached a constant temperature within three minutes after the power was turned on.

RESULTS

The calculation of the separation point, by the technique described, involves necessarily the determination of all the characteristics of the flow in the boundary layer. Some of these characteristics are noted and discussed, others may be found in the reference study by Kapur [17]. The location of the separation point is determined by extrapolation of the calculated skin friction to zero since the boundary layer equations used become singular at the separation point. Positions of the separation points are given in Table 1. All calculated results are given for a fluid stream temperature of 21°C (70°F).

Table 1. Separation points for a sphere

Above critical flow		
ΔT		α
(°C)	(°F)	
72·2	130	107·9
44·4	80	106·6
16·5	30	105·2
0	0	104·0
−44·4	−80	101·5
Below critical flow		
72·2	130	91·0
44·4	80	90·0
16·5	30	88·5
0	0	87·0
−44·4	−80	85·0

Two instances of flow about a sphere were considered. In one instance the potential velocity distribution was used and in the second an experimental distribution given by Tomotika [18], with the adverse pressure gradient beginning at 74·8°. These are called "above critical" and "below critical" flow, respectively. Thus, the term "above critical" refers to flow such that transition to turbulent flow occurs in the boundary-layer upstream of the separation point. The corresponding external flow is approximated by the potential velocity distribution and the results are appropriate to the laminar boundary layer proceeding transition.

The potential flow distribution yielded a separation point at 104°. Using the following representation for an experimental velocity distribution,

$$\frac{U_e}{U_\infty} = 1{\cdot}5\xi - 0{\cdot}3640\xi^3 + 0{\cdot}024668\xi^5, \qquad (17)$$

Tomotika [18] calculated the separation point to be at 81° using a momentum integral technique. The present calculations for this distribution yielded 87° while 85° has been measured experimentally by Fage [19].

These calculations and the experimental result of 85° correspond with the experimental results obtained with hydrogen bubbles in this study.

Microphotographs were taken of the boundary-layer flow region between 80° and 100° from the forward stagnation point. A graphical method for determining the separation point is indicated in Fig. 1. This method

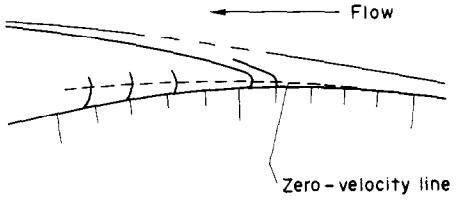

FIG. 1. Graphical procedure for extrapolating separation point from hydrogen bubble pictures.

utilizes a tracing of the bubble pattern and an extrapolated line through the loci of points of zero forward velocity in the reverse flow region. This procedure yielded the separation point of 84°. The method is considered accurate to within ±2°. It is concluded that conventional laminar flow existed over the sphere in the unheated state and that a normal separation occurred, corresponding with previous experiments and the calculations for a laminar boundary layer.

The effect on f''_w of heating and cooling the wall of a sphere with a potential flow velocity distribution is shown in Fig. 2. It is seen that small, but finite

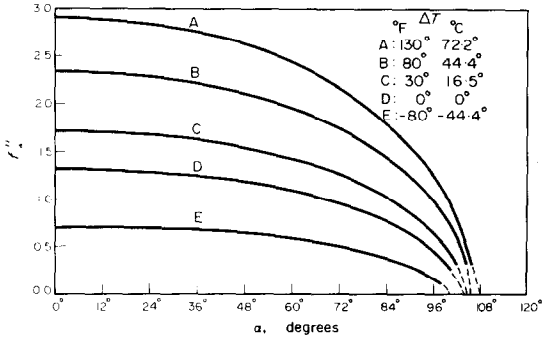

FIG. 2. The effect of heating and cooling a sphere on the velocity gradient at the wall. "Above critical" flow.

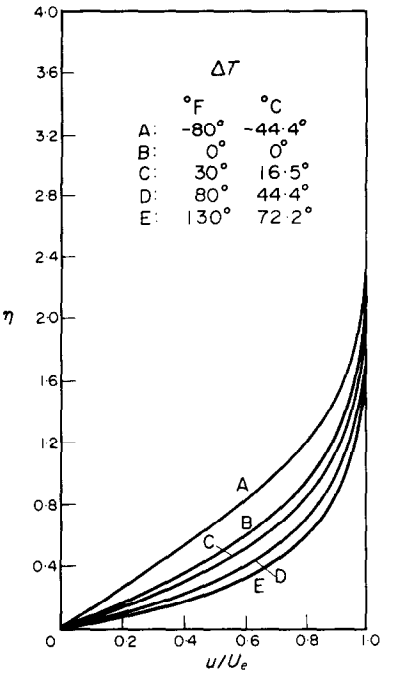

FIG. 3. Velocity profile for a heated sphere. "Above critical" flow, $\alpha = 67{\cdot}8°$.

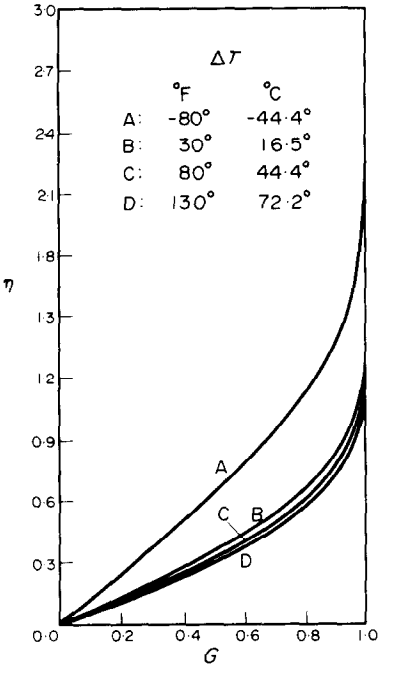

FIG. 4. Temperature profiles for a heated sphere. "Above critical" flow, $\alpha = 67{\cdot}8°$.

increases in the angle at which separation occurs are caused by increased sphere wall temperatures—an increase in angle from 102° to 108° occurring for a temperature increase of 72·2°C (130°F). Example temperature and velocity profiles are shown in Figs. 3 and 4. These boundary-layer quantities vary as would be expected and tend to confirm the results on separation. Additional profiles are given in the reference study [17].

If the sphere experiences the velocity distribution of equation (17), the results are similar to the potential flow case, the increase in separation angle for a wall temperature increase of 72·2°C being about 6° from 86 to 92°. Additional results are given in the reference study [17].

The effect of buoyancy forces were determined from the computer program. Using the definitions of positive

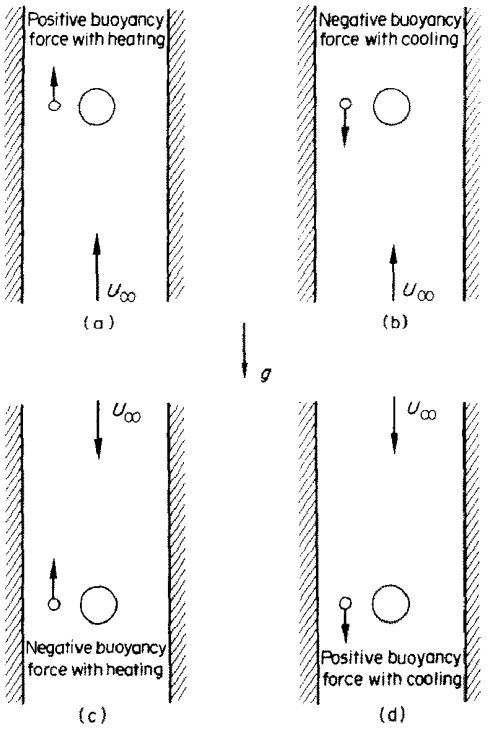

FIG. 5. Definition of positive and negative buoyancy forces.

and negative buoyancy given in Fig. 5, typical results, for the velocity distribution of equation (17), in this instance, are shown in Fig. 6. This shows relatively small buoyancy effects.

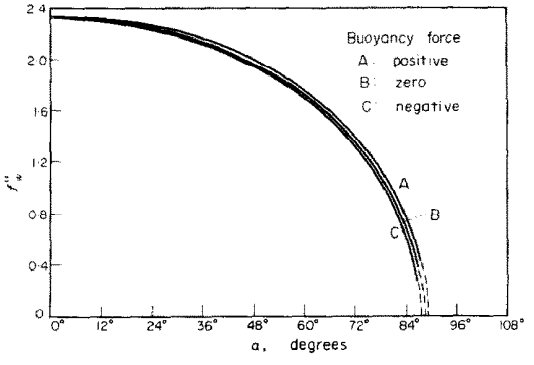

FIG. 6. The effect of buoyancy forces on the velocity gradient at the wall, when the sphere is heated. "Below critical" flow, $\Delta T = 44{\cdot}4°C$.

Good agreement was found between calculated Nusselt number, Nu_D, and the experimental results of Brown [12]. An example is shown in Fig. 7.

Difficulties in obtaining uniformly small hydrogen bubbles with the heated sphere led to the use of a shadowgraph to determine the separation point experimentally. The photographs showed several characteristics. The increase in temperature of the sphere wall for $\Delta T = 55{\cdot}5°C$ (100°F) caused the wake to become asymmetric in the vertical plane, due to buoyancy

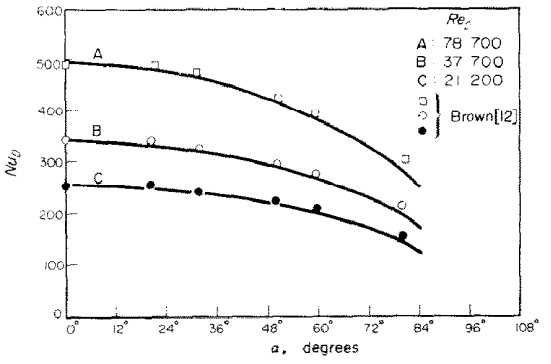

FIG. 7. Comparison of local Nusselt number with experimental results of Brown [12], $T_{wall} = 106°C$, $T_{water} = 100°C$, uniformly heated sphere.

forces. Large changes in the location of the separation point do not occur, thus, tending to confirm small changes obtained in the analytical results.

Previous numerical results obtained for a circular cylinder [13] with wall temperature different from the main stream can be compared with those shown here. Figs. 8 and 9 show the dimensionless skin friction and heat transfer in terms of the stagnation point values as a function of the dimensionless distance from the stagnation point. It is seen that the heat transfer is discernibly different between the cylinder and the sphere. A relationship for the dimensionless separation

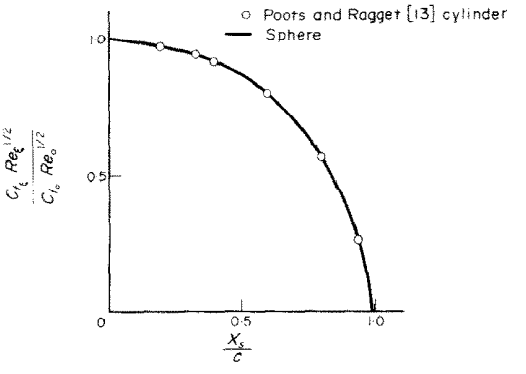

FIG. 8. Dimensionless skin friction coefficient for the ΔT's of Table 1.

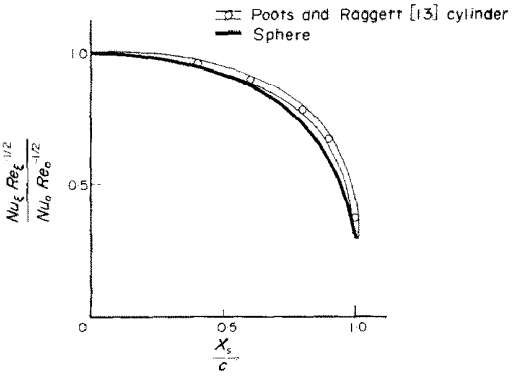

FIG. 9. Dimensionless heat-transfer coefficient for the ΔT's of Table 1.

point has been proposed for the circular cylinder by Poots and Raggett [13]. It involves the ratio of the Prandtl number evaluated at the main stream temperature and the wall temperature. This is

$$\frac{x_s}{c} = \frac{\pi}{2} + \frac{1}{4}\left(\frac{Pr_m}{Pr_w}\right)^{1/5}. \tag{18}$$

The value $\pi/2$ is the location of the beginning of the adverse pressure gradient. This correlation involving the location of the beginning of the adverse pressure gradient and the Prandtl number ratio appears to be quite good and perhaps applicable to bodies of many shapes. As seen from Fig. 10, the present study shows that more accurate relations may be

$$\text{cylinder:} \quad \frac{x_s}{c} = \pi/2 + 0{\cdot}253\left(\frac{Pr_m}{Pr_w}\right)^{0{\cdot}17} \tag{19}$$

$$\text{sphere, above critical:} \quad \frac{x_s}{c} = \pi/2 + 0{\cdot}248\left(\frac{Pr_m}{Pr_w}\right)^{0{\cdot}17} \tag{20}$$

$$\text{sphere, below critical:} \quad \frac{x_s}{c} = 1{\cdot}30 + 0{\cdot}222\left(\frac{Pr_m}{Pr_w}\right)^{0{\cdot}17} \tag{21}$$

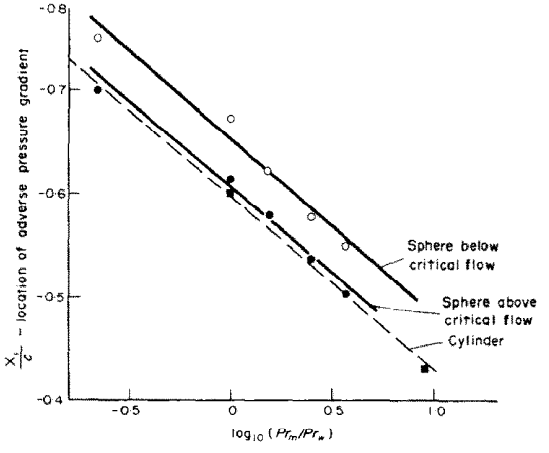

FIG. 10. Prandtl number correlation with location of the beginning of the adverse pressure gradient.

However, it is believed that the difference in the Prandtl number ratio exponent of 0·03 is likely due to differences between the Prandtl number function of temperature used in the two studies. It may be noted that the steep slope of the functions of skin friction and Nusselt number near x/x_s equal to 1 requires an accurate determination of x_s/c for an accurate prediction of skin friction coefficient or Nusselt number.

The results given herein and the correlations of equations (19), (20), and (21) can be expected to be valid for liquid flows in which boiling or freezing (cavitation or solidification) do not occur. This generality is due to the formulation of the equations and results in a dimensionless form. However, correlations of computed results, just like correlations of experimental results, cannot be extrapolated with complete confidence beyond the range of the computations (data).

CONCLUSIONS

Heating has the following significant effects:

1. It substantially increases the u component of velocity in the laminar boundary layer of water flow past a sphere. With ΔT of 72·2°C (+130°F), maximum increases in u of 50 per cent in the boundary layer occur.

2. It shifts the point of flow separation downstream from the stagnation point. The value is about 5 per cent of the distance from the forward stagnation point to the separation point for no heating, for ΔT's on the order of 55·5°C (100°F).

3. It decreases the displacement thickness and momentum thickness. With a ΔT of 72·2°C (130°F) the displacement thickness decreases by 30 per cent and the momentum thickness by 20 per cent.

4. The velocity boundary-layer thickness is changed only slightly by heating or cooling, but cooling substantially increases the thermal boundary-layer thickness.

5. Buoyancy has little effect in water flow past a sphere for ΔT's on the order of 55·5°C (100°F). For the sphere this corresponds to the ratio of the Grashof number to the square of the Reynolds number of about 0·7.

A general qualitative conclusion regarding separation is that the powerful influence of a strong adverse pressure gradient in fixing the separation point cannot be appreciably changed by moderate heating. Thus, in most instances available energy should not be used for heating in attempts to reduce adverse effects of separation.

Acknowledgement—This research was supported by the Department of Mechanical Engineering and the Division of Engineering Research, Michigan State University.

REFERENCES

1. M. Morduchow, Review of theoretical investigation on effect of heat transfer on laminar separation, *AIAA Jl* **3**(8), 1377–1385 (1965).
2. K. Stewartson, *The Theory of Laminar Boundary Layers in Compressible Fluids*. Oxford University Press, New York (1964).
3. C. R. Illingworth, The effect of heat transfer on the separation of a compressible laminar boundary layer, *Q. Jl Mech. Appl. Math.* **12**, 8 (1954).
4. G. E. Gadd, A review of theoretical work relevant to the problem of heat transfer effects on laminar separation, Aeronautical Research Council, Paper 331 (13 June, 1956).
5. N. Curle, The steady compressible laminar boundary layer, with arbitrary pressure gradient and uniform wall temperature, *Proc. R. Soc.* **A249**, 206–224 (1958).
6. G. Poots, A solution of the compressible laminar boundary layer equations with heat transfer and adverse pressure gradient, *Q. Jl Mech. Appl.* **13**, 57 (1960).
7. D. C. Baxter and I. Flügge-Lotz, The solution of compressible laminar boundary layer problems by a finite difference method, Stanford Univ. Div. of Engr. Mechanics, TRICO (15 October 1957).
8. T. Fannelop and I. Flügge-Lotz, The laminar compressible boundary layer along a wave-shaped wall, *Ing.-Arch.* **33**, 24–35 (1963).
9. H. Schuh, The solution of the laminar boundary layer equations for the flat plate for velocity and temperature fields for variable physical properties and for the dif-

fusion field at high concentration. NACA TM 1275 (May 1950).
10. O. T. Hanna and J. E. Myers, Laminar boundary layer flow and heat transfer past a flat plate for a liquid of variable viscosity, *A.I.Ch.E. Jl* **7**(3), 437–441 (1961).
11. H. A. Johnson, *Boelter Anniversary Volume: Heat Transfer, Thermodynamics and Education*, pp. 319–379. McGraw-Hill, New York (1964).
12. W. S. Brown, Forced convection heat transfer from a uniformly heated sphere to water, Ph.D. Thesis, Stanford University, Stanford, Calif. (1960).
13. G. Poots and G. F. Raggett, Theoretical results for variable property, laminar boundary layers in water with adverse pressure gradients, *Int. J. Heat and Mass Transfer* **11**, 1513–1534 (1968).
14. C. B. Millikan, The boundary layer and skin friction for a figure of revolution, *Trans. Am. Soc. Mech. Engrs* **54**, 29–43 (1932).
15. D. W. Clutter and A. M. O. Smith, Solution of the general boundary layer equations for compressible laminar flow, including transverse curvature, Douglas Aircraft Company Report No. LB31088 (February 1963).
16. D. R. Hartree and J. R. Womersley, A method for the numerical or mechanical solutions of certain types of partial differential equations, *Proc. R. Soc.* **AIGI**, 906, 353 (August 1931).
17. S. Kapur, The effect of heat transfer on the laminar boundary layer and laminar separation of water flowing past a flat plate and a sphere, Ph.D. Thesis, Michigan State University, East Lansing, Michigan (1972).
18. S. Tomotika, Laminar boundary layer on the surface of a sphere in a uniform stream, British Aeronautical Research Committee, R & M 1678 (1935).
19. A. Fage, Experiments on a sphere at critical Reynolds numbers, British Aeronautical Research Committee R & M 1766 (1936).

EFFET DE LA TEMPERATURE PARIETALE SUR LE DEVELOPPEMENT ET LA SEPARATION DE LA COUCHE-LIMITE LAMINAIRE SUR UNE SPHERE

Résumé—On présente les résultats de l'intégration numérique des équations de la couche-limite laminaire sur une sphère jusqu'au point de séparation, et les expériences effectuées sur une sphère à température constante dans l'eau à un faible nombre de Reynolds. Les résultats numériques et expérimentaux montrent tous deux qu'une augmentation de la température de la sphère au dessus de celle de l'eau environnante déplace le point de séparation laminaire légèrement vers l'arrière. L'effet des forces de gravité est très faible. On traite de l'influence du chauffage sur les profils de vitesse et de température.

Les résultats sont comparés à ceux obtenus par d'autres auteurs pour un cylindre bidimensionnel. Il est trouvé que les valeurs du transfert de chaleur et du frottement pariétal adimensionnels en fonction de la distance adimensionnelle comptée sur la paroi jusqu'au point de séparation sont semblables à celles obtenues sur un cylindre. Pour l'écoulement potentiel autour de la sphère et pour une distribution de vitesse expérimentale, on représente l'effet de la séparation par des formules incluant le rapport des nombres de Prandtl dans l'écoulement libre et à la paroi. Ces corrélations sont comparées à celles relatives à un cylindre circulaire.

EINFLUSS DER WANDTEMPERATUR AUF DAS ANWACHSEN UND DIE ABLÖSUNG DER LAMINAREN GRENZSCHICHT UM EINE KUGEL

Zusammenfassung—Ergebnisse werden gebracht für die numerische Integration der laminaren Grenzschichtgleichungen um eine Kugel bis zum Ablösepunkt und für experimentelle Untersuchungen an einer Kugel konstanter Temperatur in Wasser bei kleinen Reynolds-Zahlen. Sowohl die experimentellen als auch die numerischen Ergebnisse zeigen, daß mit dem Anwachsen der Kugeltemperatur über die des umgebenden Wassers sich der laminare Ablösepunkt leicht nach rückwärts verschiebt. Der Einfluß des Auftriebs ist sehr gering. Der Einfluß der Beheizung auf das Geschwindigkeits- und Temperaturprofil wird angegeben.

Die Ergebnisse werden verglichen mit den Ergebnissen anderer Autoren für zweidimensionale Zylinder. Der dimensionslose Wärmeübergang und die Oberflächenreibung als Funktion des dimensionslosen Abstands entlang der Wand bis zum Ablösepunkt erweisen sich als ähnlich jenen Werten, die für Zylinder erhalten wurden. Sowohl für Potentialströmung um die Kugel als auch für eine experimentelle Geschwindigkeitsverteilung, die den Einfluß der Ablösung enthält, wurden Relationen aufgestellt als Funktionen eines Verhältnisses der Freistrom- und der Wand-Prandtl-Zahl. Auch diese werden mit Korrelationen für den Kreiszylinder verglichen.

ВЛИЯНИЕ ТЕМПЕРАТУРЫ СТЕНКИ НА ОБРАЗОВАНИЕ И ОТРЫВ ЛАМИНАРНОГО ПОГРАНИЧНОГО СЛОЯ ШАРА

Аннотация — Представлены результаты численного интегрирования уравнений ламинарного пограничного слоя для шара до точки отрыва и экспериментов в воде на шаре с постоянной температурой при малом числе Рейнольдса. Как экспериментальные, так и численные результаты показывают, что повышение температуры шара выше температуры воды несколько затягивает отрыв ламинарного слоя.

Влияние выталкивающих сил очень незначительно. Представлены результаты по воздействию нагрева на профили скорости и температуры. Результаты экспериментов сравниваются с результатами, полученными другими исследователями для случая двумерного цилиндра. Обнаружено, что безразмерный теплообмен и поверхностное трение в качестве функций безразмерного расстояния вдоль стенки до точки отрыва аналогичны полученным для цилиндра. Корреляции как функции отношения функции тока к числу Прандтля на стенке получены как для случая потенциального обтекания шара, так и для экспериментального распределения скорости, что позволяет объяснить эффект отрыва. Эти результаты сравниваются с корреляциями для круглого цилиндра.